Research Square

Preprints are preliminary reports that have not undergone peer review.
They should not be considered conclusive, used to inform clinical practice,
or referenced by the media as validated information.

Asymmetric flatness prediction model for 20-high mill based on non circular arc theory

Yin-jie Ren
Jinzhong University
Dong-cheng Wang
wangdongcheng@ysu.edu.cn
Yanshan University
Hong-min Liu
Yanshan University
You-chuang Lv
Yanshan University

Article

Keywords: 20-high mill, Stainless steel thin strip, Flatness prediction, Non circular arc theory, Asymmetric flatness

Posted Date: November 5th, 2026

DOI: https://doi.org/10.21203/rs.3.rs-11347133/v1

License: This work is licensed under a Creative Commons Attribution 4.0 International License.
Read Full License

Additional Declarations: No competing interests reported.

Asymmetric flatness prediction model for 20-high mill based on non circular arc theory

Yin-jie Ren [1], Dong-cheng Wang [2,3*], Hong-min Liu [2], You-chuang Lv [2]

[1] Department of Mechanics, Jinzhong University, Jinzhong 030619, Shanxi, China
[2] National Engineering Research Center for Equipment and Technology of Cold Strip Rolling, Yanshan University, Qinhuangdao 066004, Hebei, China
[3] National Key Laboratory of Metal Forming Technology and Heavy Equipment, Xi'an 710016, Shaanxi, China
*** Corresponding author:** Dong-cheng Wang
E-mail address: wangdongcheng@ysu.edu.cn

Abstract：20-high mill in rolling stainless steel thin strip, the traditional rolling force calculation model will collapse when calculating. In order to obtain accurate rolling force in the process of asymmetric flatness prediction, this paper calculates the rolling force based on the non circular arc theory, which not only avoids the occurrence of program crash phenomenon, but also ensures the accuracy of the calculation results. On this basis, a new 20-high mill flatness prediction model is proposed to predict the flatness of cold rolled stainless steel thin strip under asymmetric rolling conditions. In addition, the influence laws of different tensile stress, friction coefficient and yield strength on the contour of rolling deformation zone and unit rolling pressure are also analyzed, which lays the foundation for the accurate prediction of 20-high mill asymmetric flatness.

Key words：20-high mill; Stainless steel thin strip; Flatness prediction; Non circular arc theory; Asymmetric flatness

1. Introduction

In the cold rolling process, the stainless steel thin strip has high yield strength and obvious work hardening. 20-high mill is very suitable for rolling stainless steel thin strip because of its small working roll diameter, high stiffness and other characteristics. In the production process of stainless steel thin strip, the problem of poor flatness (straightness) has been encountered many times. In order to reduce the occurrence of poor flatness, it is necessary to effectively control the flatness[1, 2]. The core is the flatness prediction model, how to accurately predict the flatness according to the mill equipment parameters, process parameters and flatness adjustment parameters. Ren et al[3] used the energy method to establish a new consideration of the entry and exit tensile stresses of the transverse flow of the metal model, and jointly verified the accuracy of the model through the 20-high mill rolling experiments and the finite element method, which lays the foundation for the accurate calculation of the flatness; based on the boundary integral method, a new model is established. Yuan et al[4] proposed a finite-length semi-infinite body model, based on which a 20-high mill flatness prediction model was established, and the reliability of the model was verified through very thin strip rolling experiments; Zhao et al[5] used the conjugate gradient method to solve the inter-roll pressure between the support rolls and the second intermediate rolls of a 20-high mill, and the computational accuracy of the established model was basically the same as that of the finite element method, but the model did not take strip plastic deformation into account. Did not consider the strip plastic deformation; Sun et al[6] used the elastic deformation model of the roll system, the plastic deformation model of the strip and the instability discrimination model to control the flatness

and plate convexity comprehensively; Ren et al[7] established an ultra-thin strip steel cold rolling work rolls press against the model in the 20-high mill rolling experimental process found that: when the work rolls are severely pressed against the work rolls and produce edge waves, the first intermediate rolls scuttle the rolls can not eliminate the edge wave Defects in the two ends of the work rolls are set up at each section of the tab, the use of the work rolls of the pressure against the effective suppression of strip edge thinning; based on the contact element dual-coordinate method, Yu[8] and Shin et al.[9] deduced the Sendzimir 20-high mill flatness control model. Overall, the computational efficiency of the above methods is significantly improved compared with the finite element method, but in some extreme working conditions, even the phenomenon of computational non-convergence occurs.

The traditional rolling force model generally assumes that the rolls still maintain a circular profile in the contact deformation zone, and the elastic deformation of the rolls has a large impact on the rolling pressure distribution in the contact zone, therefore, the Hitchcock theory[10] is used to correct the diameter of the rolls after the elastic deformation, and the length formula of the contact zone that takes into account the elastic flattening of the rolls is established, and the classical Bland-Ford rolling force model is developed on this basis[11]. In order to avoid the drawbacks of the Bland-Ford formula, Stone[12] established the calculation method of cold rolling average unit pressure considering the roll elastic squash. Due to the cold rolled bite angle is relatively small, and the roll diameter and thickness ratio of the rolled part is relatively large, Stone equates the rolling process to the case of compression of the block between the two flat plates. However, in the rolling of very thin strip, found that the contact length of the deformation zone is much larger than the thickness of the rolled parts, at this time the roll profile is no longer arc-shaped, the traditional rolling force model is no longer applicable.

The study of non circular arc theory, the earliest can be traced back to the early Orowan experimental work[13]. Orowan found that, under certain rolling conditions, the contact arc in the middle of the existence of a “flat zone”, the plasticity of the region under almost zero. Subsequently, Johnson and Bentall[14] on this phenomenon, Fleck and Johnson[15, 16] continued their research work, the formation of a set of theories used to solve the cold rolled foil rolling pressure and roll deformation. The most important feature of the theory is that according to the characteristics of the rolling deformation zone will be divided into three types of rolling conditions, for each type of rolling conditions using their own algorithms. That is, to calculate the rolling pressure under a particular rolling condition, it is necessary to determine which rolling condition belongs to, which requires a certain amount of experience, so that the solution process becomes cumbersome: in addition, under certain conditions, the iterative process is easy to disperse, so that the solution results are not stable[17]. In order to solve these problems, Le and Sutcliffe[18] that, in the neutral zone roll profile is not absolutely “flat”, the use of Hook's law to solve the distribution of rolling pressure in the neutral zone, and will be considered in the three rolling conditions, regardless of the rolling conditions belong to which case, a unified method of calculation, so that the robustness of the algorithm and the generalized rolling conditions. The robustness and generality of the algorithm is significantly improved. Based on Fleck's theory, there are many improved models and practical applications, Langlands et al[19, 20] used perturbation theory and Hilbert transform approximation to deal with Fleck's model; the authors of this paper[21] used segmented quadratic curves to fit pressure distributions, which led to the derivation of a set of simplified models for cold strip flat rolling; Ren et al[22, 23] found that neutral rolling was the most suitable method for cold strip rolling. found that

the elastic unloading zone in the neutral zone is negligible through test and finite element analysis, and established that the explicit expression of pressure distribution and deformation profile can be used in a simplified model for online rolling force setting; Sun et al[24] used finite element software Marc to carry out elastic-plastic finite element analysis of flat rolling, which confirmed the correctness of Fleck's theory; Feng et al[25] investigated that the Fleck model can be used to describe the asymmetric ultra-thin strip rolling driven by a single roll when the thickness is sufficiently small, which extends the scope of application of Fleck theory; some other scholars[26-27] developed a more accurate rolling force model by considering lubrication friction model on the basis of Fleck model.

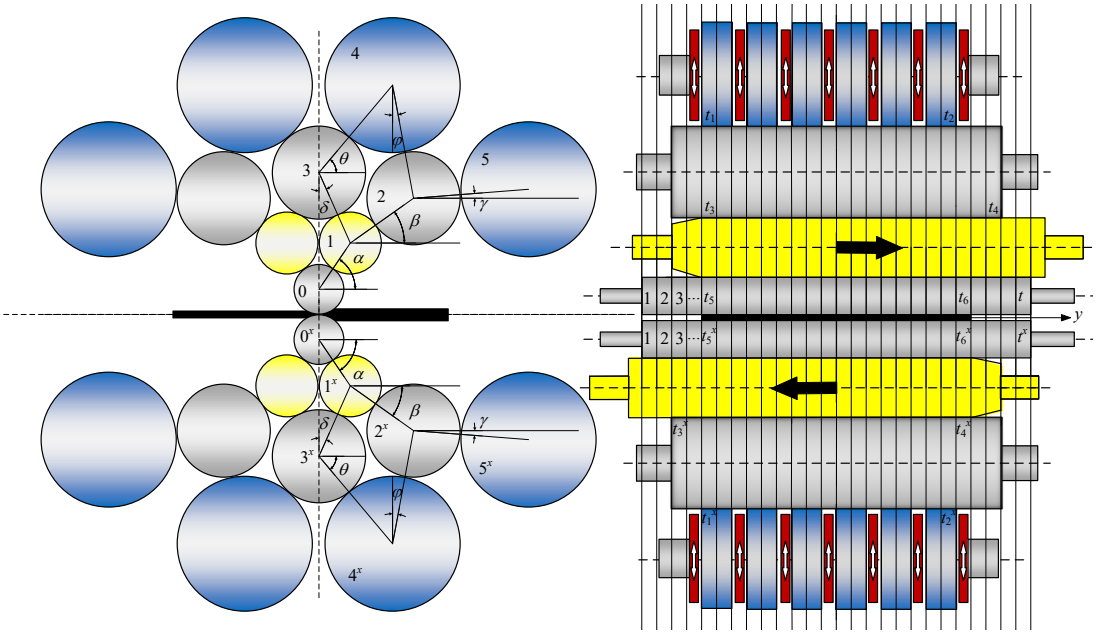
In this paper, a new 20-high mill asymmetric flatness prediction model is proposed based on the non circular arc theory, which avoids the program crash of using the traditional rolling force model in the solution process, and makes the model stability significantly improved. In Section 2, the 20-high mill asymmetric flatness prediction model based on non circular arc theory is derived in detail. In addition, the field measured flatness is utilized to verify the calculated flatness of the model in this paper. In Section 3, the effects on the contour of rolling deformation zone and unit rolling pressure are analyzed under different thicknesses, under pressure rates, tensile stresses, friction coefficients, and yield strengths, respectively, to lay the foundation for the accurate prediction of 20-high mill asymmetric flatness. Finally, Section 4 is the main conclusion of this paper.

2 20-high mill asymmetric flatness prediction model based on non circular arc theory

2.1 Division of roll system units

The number and angle of each roll of Sendzimir 20-high mill are shown in Fig. 1(a). In the upper roll system, the angle between the center point of the cross section of roll 0 and roll 1 and the horizontal direction is α, the angle between the center point of the cross section of roll 1 and roll 3 and the vertical direction is δ, the angle between the center point of the cross section of roll 1 and roll 2 and the horizontal direction is β, the angle between the center point of the cross section of roll 3 and roll 4 and the horizontal direction is θ, the angle between the center point of the cross section of roll 2 and roll 4 and the vertical direction is φ, and the angle between the center point of roll 2 and roll 5 and the horizontal direction is γ. Under the roll system of the roll marking on the corner mark for *x*, under the roll system of the angle between the rolls and the roll system is equal, can be analogized to get so do not repeat.

Strip and roll system unit is divided as shown in Fig. 1(b), the origin of the coordinates *O* selected in the strip midpoint. Rolls and strips as a whole for unit division, divided into t units. The width of each unit is Δy_i (i=1,2,...,t) ,and the coordinates of its center point are y_i (i=1,2,...,t) . Among them, the 4 roll and the 3 roll contact part of the beginning unit number is t_1,the end of the unit number is t_2； 3 roll and the 1 roll contact part of the beginning unit number is t_3,the end of the unit number is t_4； 1 roll and the 0 roll contact part of the beginning unit number is 1, the end of the unit number is t； the work of the roll and the strip contact part of the beginning unit number is t_5,the end of the unit number is t_6.The lower roll system unit number on the corner of the *x*, can be obtained by analogy, so do not repeat.



(a)Number and angle of each roll; (b)strip and roll unit division;

Fig. 1 Schematic diagram of roll system angle, numbering and unit division

The forces on the rolls are shown in Fig. 2. p_i denotes the rolling pressure per unit width on unit i; the pressure between each roll is q_{01i}, q_{12i}, q_{13i}, q_{24i}, q_{25i} and q_{34i}. Where, q_{XYi} indicates the contact pressure on the unit i between roll X and roll Y. The length of roll body of roll 0 is L_w; the length of roll body of roll 4 and 5 is L_b; the length of roll body of roll 1 is L_{m1}; the length of roll body of roll 2 and 3 is L_{m2} The lower roller system and the upper roller system of the pressure between the rollers on the corner labeled *x*, can be obtained by analogy, so do not repeat.

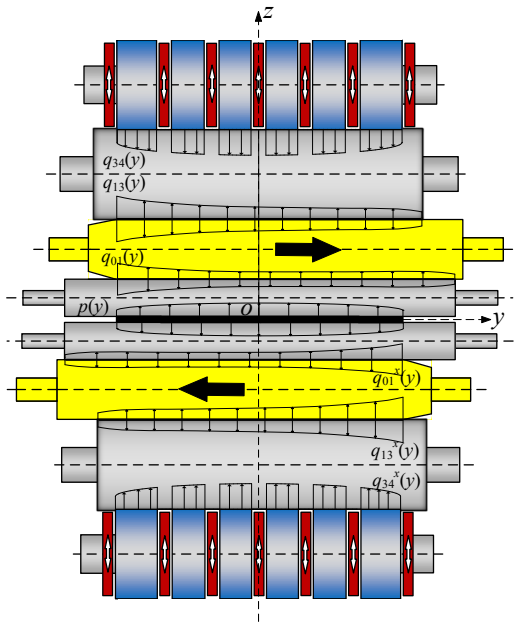


Fig. 2 Schematic diagram of the force acting on the roller system of the Sendzimir 20-high mill

2.2 Strip plastic deformation modeling

The strip-element variational method[27] is an efficient method for calculating strip plastic deformation, based on the variational method and introducing the idea of splitting strips of the strip-element method, which can more accurately describe the distribution of parameters in the direction of the strip width, and the distribution of the exit transverse displacements can be obtained at one

time by solving only a set of linear equations.

When performing strip plastic deformation calculations, the strip width B is divided into n independent units within the deformation zone length g, and the exit transverse displacement $u_j(j=0\sim n)$ of the strip unit knuckle line needs to be taken as an unknown quantity. For ease of presentation, the strip unit knuckle lines are renumbered as shown in Fig. 3. The two section lines corresponding to unit t_5 are numbered 0 and 1, the two section lines corresponding to unit t_6 are numbered $n-1$ and n, and the numbering of the section lines of other units can be obtained by analogy. The transverse coordinates of the cell section lines are denoted as y_i, and the width of the strip element cell is $\Delta y_i = y_i - y_{i-1}$.

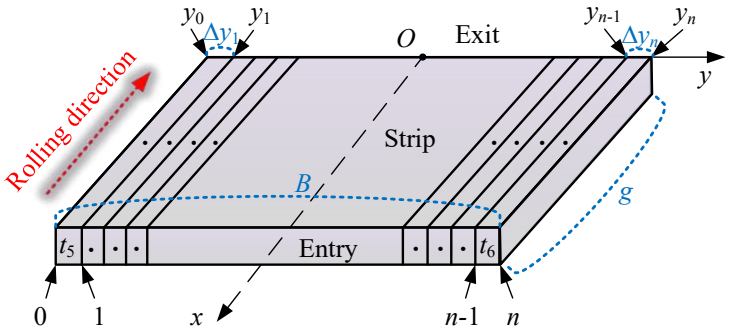


Fig 3 Correspondence between unit section line numbering and unit numbering

$$\begin{cases} \left(\alpha_{t_5}-e_{\mathrm{b}}\right)u_0+\beta_{t_5}u_1+e_{\mathrm{b}}u_n=-\sigma_{\mathrm{s}}/\sqrt{3}+c_{t_5} \\ \vdots \\ \beta_i u_{j-1}+\left(\alpha_i+\alpha_{i+1}\right)u_j+\beta_{i+1}u_{j+1} \\ =c_{i+1}-c_i,\quad \left(j=1,2,\ldots,n-1;i=j-1+t_5\right) \\ \vdots \\ e_{\mathrm{b}}u_0+\beta_{t_6}u_{n-1}+\left(\alpha_{t_6}-e_{\mathrm{b}}\right)u_n=\sigma_{\mathrm{s}}/\sqrt{3}-c_{t_6} \end{cases} \tag{1}$$

Where, $\alpha_{t_5}\sim\alpha_{t_6}$, $\beta_{t_5}\sim\beta_{t_6}$ is the strip export thickness transverse distribution of parameters; $e_{\mathrm{b}}=\dfrac{E_{\mathrm{s}}}{(1-\upsilon_{\mathrm{s}}^2)B}$; $c_i=\dfrac{E_{\mathrm{s}}}{1-\upsilon_{\mathrm{s}}^2}\left(1+\dfrac{h_{1i}}{\bar{h}_1}-\dfrac{h_{0i}}{\bar{h}_0}-\dfrac{l_{0i}}{\bar{l}_0}\right),(i=t_5\sim t_6)$; E_{s}, υ_{s} is the strip modulus of elasticity and Poisson's ratio, respectively; $\bar{h}_0$, $\bar{h}_1$ is the strip into the export average thickness, respectively; h_{0i}, h_{1i} is the strip into the export thickness of transverse distribution, respectively; $\bar{l}_0$, l_{0i} is the strip entry average length and the entry length of the transverse distribution, respectively; σ_{s} is the strip deformation resistance.

The lateral distribution of entry and exit tensile stresses is indicated below:

$$\sigma_{0i}=\bar{\sigma}_0+\frac{E_{\mathrm{s}}}{1-\upsilon_{\mathrm{s}}^2}\left[1+\frac{h_{1i}\bar{h}_0(1+u_j')}{h_{0i}\bar{h}_1(1+\dfrac{u_n-u_0}{B})}-\frac{l_{0i}}{\bar{l}_0}\right],(i=t_5\sim t_6,j=0\sim n) \tag{2}$$

$$\sigma_{1i}=\bar{\sigma}_1+\frac{E_s}{1-\upsilon_s^2}\left[1+\frac{h_{1i}}{\bar{h}_1}-\frac{h_{0i}}{\bar{h}_0}-\frac{l_{0i}}{\bar{l}_0}+u'_j-\frac{u_n-u_0}{B}\right],(i=t_5\sim t_6,j=0\sim n) \tag{3}$$

Where, $\bar{\sigma}_0$, $\bar{\sigma}_1$ are the average entry and exit tensile stresses of the strip, respectively; $\bar{\sigma}_1=T_1/\left(B\bar{h}_1\right)$, $\bar{\sigma}_0=T_0/\left(B\bar{h}_0\right)$; T_0 , T_1 are the total entry and exit tensions, respectively; σ_{0i} , σ_{1i} are the transverse distributions of the entry and exit tensile stresses, respectively; $u'_j=K_i\,\mathrm{csch}\left(K_i\Delta y_i\right)\left[-\mathrm{ch}(\frac{K_i\Delta y_i}{2})u_{j-1}+\mathrm{ch}(\frac{K_i\Delta y_i}{2})u_j\right]$; K_i are the parameters corresponding to the distribution of the strip exit thicknesses.

2.3 Calculation model of unit rolling force based on non circular arc theory

As shown in Fig. 4, the rolling direction is taken as the *x*-axis, the strip width direction is taken as the *y*-axis, and the strip thickness direction is taken as the *z*-axis. Based on Fleck theory, the non circular arc profile makes the deformation zone divided into 5 parts: elastic slip at entry, plastic slip at entry, sticking region, elastic slip at exit, and plastic slip at exit.

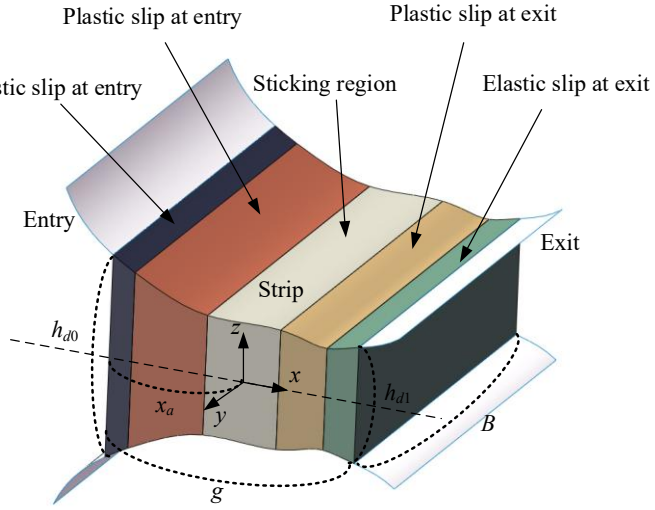


Fig. 4 Non circular phenomenon in rolling deformation zone

2.3.1 Elastic compression of rolls with contour equations

$$h_d=h_{d0}+2\sqrt{R_0^2-x_a^2}-2\sqrt{R_0^2-x^2}+2\varpi \tag{4}$$

Where, h_{d0} is the thickness of the strip entry side of the deformation zone; R_0 is the radius of roll 0; x_a is the distance from the strip entry to the *z*-axis in the deformation zone; ϖ is the amount of elastic flattening of the roll caused by the unit rolling force p_d, and the specific expression is shown in the literature[21].

2.3.2 Elastic slip at entry and exit

The relationship between frictional stress τ_d and unit rolling force p_d is adopted as Coulomb's friction law, then the differential equations of unit rolling force in the entry and exit

elastic slip are:

$$\begin{cases} \dfrac{\mathrm{d}p_d}{\mathrm{d}x} = -\dfrac{E_s}{\left(1-\upsilon_s^2\right)h_d}\dfrac{\mathrm{d}h_d}{\mathrm{d}x} + \dfrac{\upsilon_s}{1-\upsilon_s}\dfrac{2\mu p_d}{h_d} + \dfrac{\upsilon_s}{1-\upsilon_s}\dfrac{\left(p_d+\sigma\right)}{h_d}\dfrac{\mathrm{d}h_d}{\mathrm{d}x} \\ \dfrac{\mathrm{d}p_d}{\mathrm{d}x} = -\dfrac{E_s}{\left(1-\upsilon_s^2\right)h_d}\dfrac{\mathrm{d}h_d}{\mathrm{d}x} - \dfrac{\upsilon_s}{1-\upsilon_s}\dfrac{2\mu p_d}{h_d} + \dfrac{\upsilon_s}{1-\upsilon_s}\dfrac{\left(p_d+\sigma\right)}{h_d}\dfrac{\mathrm{d}h_d}{\mathrm{d}x} \end{cases} \tag{5}$$

Where, h_d is the strip thickness distribution in the deformation zone; p_d is the unit rolling force distribution in the deformation zone; μ is the friction coefficient; σ is the normal stress in the rolling direction in the deformation zone.

2.3.3 Plastic slip at entry and exit

Using the Mises yield criterion and the Coulomb friction law for the relationship between friction stress τ_d and unit rolling force p_d, the differential equations for the unit rolling force in the entry and exit plastic slip are:

$$\begin{cases} \dfrac{\mathrm{d}p_d}{\mathrm{d}x} = \dfrac{2}{\sqrt{3}}\dfrac{\sigma_s}{h_d}\dfrac{\mathrm{d}h_d}{\mathrm{d}x} + \dfrac{2\mu p_d}{h_d} \\ \dfrac{\mathrm{d}p_d}{\mathrm{d}x} = \dfrac{2}{\sqrt{3}}\dfrac{\sigma_s}{h_d}\dfrac{\mathrm{d}h_d}{\mathrm{d}x} - \dfrac{2\mu p_d}{h_d} \end{cases} \tag{6}$$

2.3.4 Sticking region

In the sticking region, the differential equation for the unit rolling force in the entry and exit plastic slip is:

$$\frac{\mathrm{d}p_d}{\mathrm{d}x} = \frac{E_s E_0}{E_s\left(1-2\upsilon_0\right)\left(1+\upsilon_0\right) - 2E_0\left(1-2\upsilon_s\right)\left(1+\upsilon_s\right)}\frac{\mathrm{d}h_d}{h_d\mathrm{d}x} \tag{7}$$

$$\tau_d = \left[\frac{E_s E_0}{2E_s\left(1-2\upsilon_0\right)\left(1+\upsilon_0\right) - 4E_0\left(1-2\upsilon_s\right)\left(1+\upsilon_s\right)} - \frac{\sigma_s}{\sqrt{3}}\right]\frac{\mathrm{d}h_d}{\mathrm{d}x} \tag{8}$$

Where, E_0 is the modulus of elasticity of roll 0; υ_0 is the Poisson's ratio of roll 0.

Solving the differential equation Eq. (5), Eq. (6) and Eq. (7), the distribution of unit rolling force p_d in the whole deformation zone can be obtained. The friction stress τ_d in the neutral zone is calculated according to Eq. (8).

2.4 Elastic deformation model of roll system

The influence function method is a discretization method, also known as the split model method. After the continuous improvement of many scholars [28-30], the method has been relatively mature, and its calculation speed and accuracy can meet the engineering needs, this paper will be used as the roll system elastic deformation model.

First listed 0 and 1, 0^x and 1^x, 1 and 2, 1^x and 2^x, 1 and 3, 1^x and 3^x, 2 and 4, 2^x and 4^x, 2 and 5, 2^x and 5^x, 3 and 4, 3^x and 4^x number of rolls in the direction of the line connecting the center point of the cross-section of the rolls in the inter-roll deformation coordination equation as Eq. (9):

$$
\begin{cases}
f_{0i} = f_{1i} + \gamma_{01i} q_{01i} + \Delta D_{01i}, (i = 1 \sim t) \\
f_{0i}{}^{x} = f_{1i}{}^{x} + \gamma_{01i}{}^{x} q_{01i}{}^{x} + \Delta D_{01i}{}^{x}, (i = 1 \sim t^{x}) \\
\cos(\alpha - \beta) f_{1i} = f_{2i} + \gamma_{12i} q_{12i} + \Delta D_{12i}, (i = t_3 \sim t_4) \\
\cos(\alpha - \beta) f_{1i}{}^{x} = f_{2i}{}^{x} + \gamma_{12i}{}^{x} q_{12i}{}^{x} + \Delta D_{12i}{}^{x}, (i = t_3{}^{x} \sim t_4{}^{x}) \\
\sin(\alpha - \delta) f_{1i} = f_{3i} + \gamma_{13i} q_{13i} + \Delta D_{13i}, (i = t_3 \sim t_4) \\
\sin(\alpha - \delta) f_{1i}{}^{x} = f_{3i}{}^{x} + \gamma_{13i}{}^{x} q_{13i}{}^{x} + \Delta D_{13i}{}^{x}, (i = t_3{}^{x} \sim t_4{}^{x}) \\
\sin(\beta - \varphi) f_{2i} = \cos\varphi f_{4i} + \gamma_{24i} q_{24i} + \Delta D_{24i}, (i = t_1 \sim t_2) \\
\sin(\beta - \varphi) f_{2i}{}^{x} = \gamma_{24i}{}^{x} q_{24i}{}^{x} + \Delta D_{24i}{}^{x}, (i = t_1{}^{x} \sim t_2{}^{x}) \\
\cos(\beta - \gamma) f_{2i} = \gamma_{25i} q_{25i} + \Delta D_{25i}, (i = t_1 \sim t_2) \\
\cos(\beta - \gamma) f_{2i}{}^{x} = \gamma_{25i}{}^{x} q_{25i}{}^{x} + \Delta D_{25i}{}^{x}, (i = t_1{}^{x} \sim t_2{}^{x}) \\
\sin(\theta - \delta) f_{3i} = \sin\theta f_{4i} + \gamma_{34i} q_{34i} + \Delta D_{34i}, (i = t_1 \sim t_2) \\
\sin(\theta - \delta) f_{3i}{}^{x} = \gamma_{34i}{}^{x} q_{34i}{}^{x} + \Delta D_{34i}{}^{x}, (i = t_1{}^{x} \sim t_2{}^{x})
\end{cases} \tag{9}
$$

Where, f_{Xi} indicates that the X number of rolls and mutual contact with the rolls in the direction of the center point of the cross-section of the line on the i unit deflection, f_{4i} is the 4 rolls in the vertical direction of any unit deflection, ΔD_{XYi} indicates that the X number of rolls and the Y number of rolls in the i unit of the rolls of the original gap or convexity, γ_{XYi} indicates that the X number of rolls and the Y number of rolls in the i unit of elasticity flattening influence coefficients.

0, 0^x, 1, 1^x roll force and moment balance equation is:

$$
\begin{cases}
2\sin\alpha \sum_{i=1}^{t} (q_{01i} \Delta y_i) = \sum_{i=t_5}^{t_6} (p_i \Delta y_i) \\
2\sin\alpha \sum_{i=1}^{t} (q_{01i} \Delta y_i y_i) = \sum_{i=t_5}^{t_6} (p_i \Delta y_i y_i) \\
2\sin\alpha \sum_{i=1}^{t^x} (q_{01i}{}^{x} \Delta y_i) = \sum_{i=t_5{}^{x}}^{t_6{}^{x}} (p_i \Delta y_i) \\
2\sin\alpha \sum_{i=1}^{t^x} (q_{01i}{}^{x} \Delta y_i y_i) = \sum_{i=t_5{}^{x}}^{t_6{}^{x}} (p_i \Delta y_i y_i) \\
\sin\beta \sum_{i=t_3}^{t_4} (q_{12i} \Delta y_i) + \cos\delta \sum_{i=t_3}^{t_4} (q_{13i} \Delta y_i) = \sin\alpha \sum_{i=1}^{t} (q_{01i} \Delta y_i) \\
\sin\beta \sum_{i=t_3}^{t_4} (q_{12i} \Delta y_i y_i) + \cos\delta \sum_{i=t_3}^{t_4} (q_{13i} \Delta y_i y_i) = \sin\alpha \sum_{i=1}^{t} (q_{01i} \Delta y_i y_i) \\
\cos\beta \sum_{i=t_3}^{t_4} (q_{12i} \Delta y_i) - \sin\delta \sum_{i=t_3}^{t_4} (q_{13i} \Delta y_i) = \cos\alpha \sum_{i=1}^{t} (q_{01i} \Delta y_i) \\
\cos\beta \sum_{i=t_3}^{t_4} (q_{12i} \Delta y_i y_i) - \sin\delta \sum_{i=t_3}^{t_4} (q_{13i} \Delta y_i y_i) = \cos\alpha \sum_{i=1}^{t} (q_{01i} \Delta y_i y_i) \\
\sin\beta \sum_{i=t_3{}^{x}}^{t_4{}^{x}} (q_{12i}{}^{x} \Delta y_i) + \cos\delta \sum_{i=t_3{}^{x}}^{t_4{}^{x}} (q_{13i}{}^{x} \Delta y_i) = \sin\alpha \sum_{i=1}^{t^x} (q_{01i}{}^{x} \Delta y_i) \\
\sin\beta \sum_{i=t_3{}^{x}}^{t_4{}^{x}} (q_{12i}{}^{x} \Delta y_i y_i) + \cos\delta \sum_{i=t_3{}^{x}}^{t_4{}^{x}} (q_{13i}{}^{x} \Delta y_i y_i) = \sin\alpha \sum_{i=1}^{t^x} (q_{01i}{}^{x} \Delta y_i y_i) \\
\cos\beta \sum_{i=t_3{}^{x}}^{t_4{}^{x}} (q_{12i}{}^{x} \Delta y_i) - \sin\delta \sum_{i=t_3{}^{x}}^{t_4{}^{x}} (q_{13i}{}^{x} \Delta y_i) = \cos\alpha \sum_{i=1}^{t^x} (q_{01i}{}^{x} \Delta y_i) \\
\cos\beta \sum_{i=t_3{}^{x}}^{t_4{}^{x}} (q_{12i}{}^{x} \Delta y_i y_i) - \sin\delta \sum_{i=t_3{}^{x}}^{t_4{}^{x}} (q_{13i}{}^{x} \Delta y_i y_i) = \cos\alpha \sum_{i=1}^{t^x} (q_{01i}{}^{x} \Delta y_i y_i)
\end{cases} \tag{10}
$$

The equations of force and moment balance for rolls 2, 2^x, 3, and 3^x are:

$$\begin{cases}
\sin\gamma\sum_{i=t_1}^{t_2}(q_{25i}\Delta y_i)+\cos\varphi\sum_{i=t_1}^{t_2}(q_{24i}\Delta y_i)=\sin\beta\sum_{i=t_3}^{t_4}(q_{12i}\Delta y_i)\\
\sin\gamma\sum_{i=t_1}^{t_2}(q_{25i}\Delta y_i y_i)+\cos\varphi\sum_{i=t_1}^{t_2}(q_{24i}\Delta y_i y_i)=\sin\beta\sum_{i=t_3}^{t_4}(q_{12i}\Delta y_i y_i)\\
\cos\gamma\sum_{i=t_1}^{t_2}(q_{25i}\Delta y_i)-\sin\varphi\sum_{i=t_1}^{t_2}(q_{24i}\Delta y_i)=\cos\beta\sum_{i=t_3}^{t_4}(q_{12i}\Delta y_i)\\
\cos\gamma\sum_{i=t_1}^{t_2}(q_{25i}\Delta y_i y_i)-\sin\varphi\sum_{i=t_1}^{t_2}(q_{24i}\Delta y_i y_i)=\cos\beta\sum_{i=t_3}^{t_4}(q_{12i}\Delta y_i y_i)\\
\sin\gamma\sum_{i=t_1^x}^{t_2^x}(q_{25i}{}^x\Delta y_i)+\cos\varphi\sum_{i=t_1^x}^{t_2^x}(q_{24i}{}^x\Delta y_i)=\sin\beta\sum_{i=t_3^x}^{t_4^x}(q_{12i}{}^x\Delta y_i)\\
\sin\gamma\sum_{i=t_1^x}^{t_2^x}(q_{25i}{}^x\Delta y_i y_i)+\cos\varphi\sum_{i=t_1^x}^{t_2^x}(q_{24i}{}^x\Delta y_i y_i)=\sin\beta\sum_{i=t_3^x}^{t_4^x}(q_{12i}{}^x\Delta y_i y_i)\\
\cos\gamma\sum_{i=t_1^x}^{t_2^x}(q_{25i}{}^x\Delta y_i)-\sin\varphi\sum_{i=t_1^x}^{t_2^x}(q_{24i}{}^x\Delta y_i)=\cos\beta\sum_{i=t_3^x}^{t_4^x}(q_{12i}{}^x\Delta y_i)\\
\cos\gamma\sum_{i=t_1^x}^{t_2^x}(q_{25i}{}^x\Delta y_i y_i)-\sin\varphi\sum_{i=t_1^x}^{t_2^x}(q_{24i}{}^x\Delta y_i y_i)=\cos\beta\sum_{i=t_3^x}^{t_4^x}(q_{12i}{}^x\Delta y_i y_i)\\
2\sin\theta\sum_{i=t_1}^{t_2}(q_{34i}\Delta y_i)=2\cos\delta\sum_{i=t_3}^{t_4}(q_{13i}\Delta y_i)\\
2\sin\theta\sum_{i=t_1}^{t_2}(q_{34i}\Delta y_i y_i)=2\cos\delta\sum_{i=t_3}^{t_4}(q_{13i}\Delta y_i y_i)\\
2\sin\theta\sum_{i=t_1^x}^{t_2^x}(q_{34i}{}^x\Delta y_i)=2\cos\delta\sum_{i=t_3^x}^{t_4^x}(q_{13i}{}^x\Delta y_i)\\
2\sin\theta\sum_{i=t_1^x}^{t_2^x}(q_{34i}{}^x\Delta y_i y_i)=2\cos\delta\sum_{i=t_3^x}^{t_4^x}(q_{13i}{}^x\Delta y_i y_i)
\end{cases}\tag{11}$$

From the point of view of elastic deformation of the roll system, the strip exit thickness distribution is expressed as:

$$h_{1i}=s_0+2\sin\alpha\left(f_{0i}+f_{0i}{}^x\right)+\delta_{0i}+\delta_{0i}{}^x+\frac{\Delta D_{0i}+\Delta D_{0i}{}^x}{2},(i=t_5\sim t_6)\tag{12}$$

Where, s_0 is the value of the no-load roll gap; ΔD_{0i}, $\Delta D_{0i}{}^x$ respectively for the 0, 0^x roll roll type distribution value; δ_{0i}, $\delta_{0i}{}^x$ respectively for the 0, 0^x roll and the elastic flattening between the rolled parts.

When analyzing the flatness problem, usually the input parameters do not include the unloaded roll gap, but directly given the average thickness of the strip exit $\bar{h}_1$, then it is necessary to establish a new linear equation. According to the condition that the average thickness of the strip exit is equal to $\bar{h}_1$, the discrete integrals are performed on the left and right sides of Eq. (12), and the left side of the equation is integrated as:

$$\sum_{i=t_5}^{t_6}(h_{1i}\cdot\Delta y_i)=\bar{h}_1 B\tag{13}$$

After integrating the right side of the equation of Eq. (12), Eq. (13) is substituted to obtain Eq. (14).

$$\begin{aligned} & s_0 B + 2\sin\alpha\left(\sum_{i=t_5}^{t_6} f_{0i}\Delta y_i + \sum_{i=t_5^x}^{t_6^x} f_{0i}{}^x \Delta y_i\right) + \sum_{i=t_5}^{t_6} \delta_{0i}\Delta y_i + \sum_{i=t_5^x}^{t_6^x} \delta_{0i}{}^x \Delta y_i \\ & = \bar{h}_1 B - \frac{1}{2}\left[\sum_{i=t_5}^{t_6} (\Delta D_{0i}\Delta y_i) + \sum_{i=t_5^x}^{t_6^x} (\Delta D_{0i}{}^x \Delta y_i)\right] \end{aligned} \tag{14}$$

2.5 Overall calculation flow

The overall computational flow is shown in Fig. 5. The iterative method is used in the calculation. The maximum difference η_1 between the calculated value of inter-roll pressure and the iterative value and the maximum difference η_2 between the two adjacent exit thicknesses are taken as 0.01 N/mm and 0.1 μm, respectively. the inter-roll pressure distribution and the lateral distribution of the strip exit thickness are updated by the exponential smoothing method, which is shown in Eq. (15).

$$\begin{cases} q_i^{k+1} = q_i^k + \chi_1(q_i^{*k} - q_i^k) \\ h_{1i}^{k+1} = h_{1i}^k + \chi_2(h_{1i}^{*k} - h_{1i}^k) \end{cases} \tag{15}$$

Where: $k+1$, k are the $k+1$ st value and the k st value, respectively; * indicates the iteration value, and without * is the calculated value; χ_1 is the smoothing constant for updating the pressure between rolls; χ_2 is the smoothing constant for updating the strip exit thickness;

As shown in Fig. 5, when the judgment conditions are met to jump out of the loop, the transverse distribution of residual stress σ_{ci} is firstly found by Eq. (16), and then the transverse distribution of flatness value F_i is found by Eq. (17).

$$\sigma_{ci} = \sigma_{1i} - \bar{\sigma}_1, (i = t_5 \sim t_6) \tag{16}$$

$$F_i = -\frac{\sigma_{ci}\left(1-\upsilon_s^2\right)}{E_s} \times 10^5, (i = t_5 \sim t_6) \tag{17}$$

2.6 Model validation

In order to compare the stability and accuracy of the rolling force calculation model using traditional rolling force calculation model and the rolling force calculation model based on non circular theory, the rolling data in the literature [31] are used for simulation respectively. Literature used in the 20-high mill work roll material for the M2 (grade W6Mo5Cr4V2), the work roll diameter of 16 mm, the roll length of 280 mm, rolling 304 stainless steel strip, the maximum rolling force of the mill is 400 KN.

Table 1 Technology parameters

Example	Width (mm)	Entry thickness (mm)	Exit thickness (mm)	Entry tension (KN)	Exit tension (KN)	Deformation resistance (MPa)	Measured rolling force (KN)
1	150	0.049	0.038	1.454	0.969	602	80
2	200	0.038	0.032	2.015	0.851	701	92

When using the traditional rolling force model to calculate examples 1 and 2, due to the strip thickness is very thin, the traditional rolling force model calculation program has collapsed. Based

on the non circular arc theory of rolling force model calculation program, but did not collapse, the calculated example 1 rolling force of 74 KN, example 2 rolling force of 87 KN, and the measured rolling force is very close.

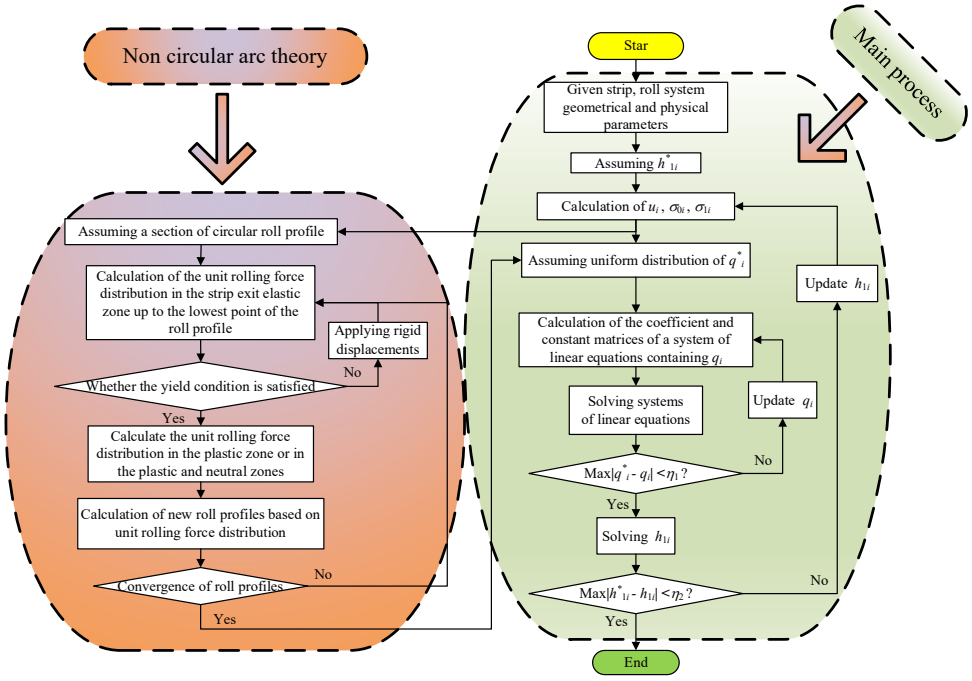


Fig. 5 Overall calculation process

3. Results and discussion

20-high mill in the production of cold rolled stainless steel strip, the contact deformation zone arc length is generally much larger than the strip thickness, the elastic flattening of the work roll leads to the work roll profile into a non circular arc profile. And because the work roll flattening has a great influence on the distribution of rolling pressure, and rolling pressure is related to the accuracy of the 20-high mill asymmetric flatness prediction model. In order to grasp the 20-high mill asymmetric flatness prediction model in the rolling deformation zone contour and unit rolling pressure change rule. This section analyzes in different thicknesses, under pressure rate, tensile stress, friction coefficient, yield strength, the rolling deformation zone contour and the unit rolling pressure, to accurately forecast the 20-high mill asymmetric flatness to lay the foundation.

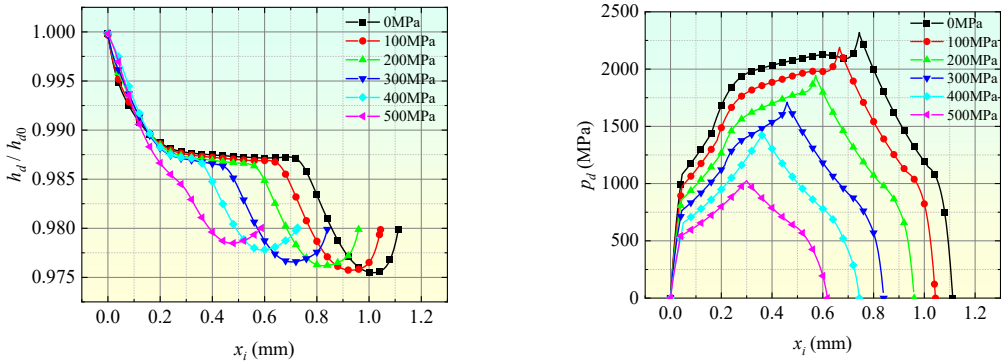
3.1 Different tensile stresses

The entry and exit tensile stresses of six kinds of strips were selected as 0, 100, 200, 300, 400 and 500 MPa respectively, given the rolling process parameters: strip thickness of 0.08 mm, the undercutting rate was set to 2 %, the modulus of elasticity of rolls 0 and 0^x was 236,000 MPa, Poisson's ratio of rolls 0 and 0^x was 0.3, the strip elasticity was 194,020 MPa, strip Poisson's ratio is 0.28, strip yield strength is 1000 MPa, coefficient of friction is 0.1, assuming that the incoming material cross-section shape is straight, the taper of rolls No.1 and 1^x is 0 % and the length of the taper is 0 mm, and the ASU is not adjusted.

Fig. 6 shows the contour of the contact deformation zone and the distribution of the unit rolling pressure for different tensile stresses applied. When the strip thickness is the same, when the strip entry and exit tensile stresses are 0 MPa, as shown in Fig. 6(a), the contact contour presents a non

circular arc shape, and the plastic depression in the middle region of the deformation zone is very small, and a long neutral zone can be observed, which indicates that the deformation zone contour at this time has already appeared an obvious neutral zone. When the strip entry and exit tensile stresses are 500 MPa, the contact profile maintains the arc shape, and the plastic depression along the whole deformation zone is relatively obvious, and there is no neutral zone. As the strip entry and exit tensile stresses increase, the proportion of the neutral zone in the deformation zone decreases, and the contact profile gradually changes from a non circular arc shape to a circular arc shape. As shown in Fig. 6(b), when the strip entry and exit tensile stresses are gradually increased from 0 MPa to 500 MPa, the unit rolling pressure in the deformation zone gradually decreases, and the unit rolling pressure is gradually changed from the elliptical distribution mentioned in the Hertz theory to the traditional “peak” distribution. It was found that equal application of the strip entry and exit tensile stresses is equivalent to a reduction in the yield strength of the strip by tensile stresses.

3.2 Different friction coefficients



(a)Ratio of strip thickness in the deformation zone to the entry thickness

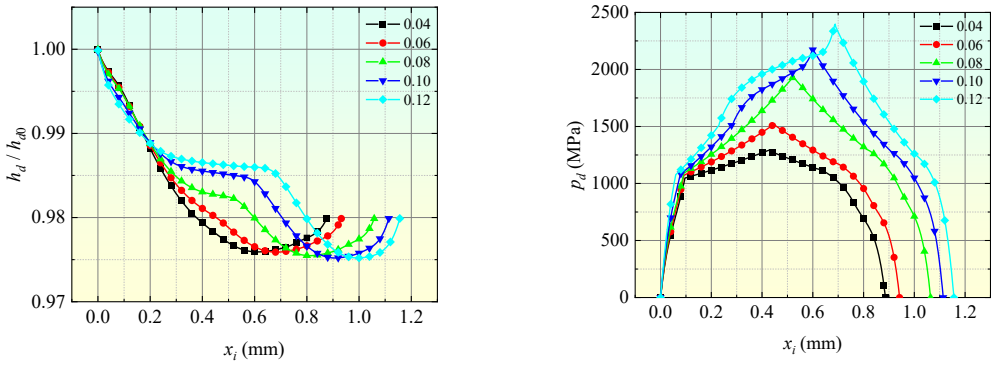
(b)unit rolling pressure

Fig. 6 Contours of deformation zone and unit rolling pressure at different tensile stresses

Five friction coefficients of 0.04, 0.06, 0.08, 0.10, and 0.12 were selected, given the rolling process parameters: strip thickness of 0.12 mm, the undercutting rate was set to 2 %, the modulus of elasticity of the 0 and 0^x rolls was 236000 MPa, the Poisson's ratio of the 0 and 0^x rolls was 0.3, and the strip elasticity modulus was 194020 MPa, Poisson's ratio was 0.28. The strip yield strength was 1000 MPa, the strip yield strength was 0.28. The strip yield strength was 1,000 MPa. The strip yield strength is 1000 MPa, the strip entry and exit tensile stresses are both 0 MPa, assuming that the incoming section shape is straight, the taper of rolls 1 and 1^x is 0 % and the taper length is also 0 mm, and the ASU is not adjusted.

Fig. 7 shows the contour of the contact deformation zone and the distribution of the unit rolling pressure when different friction coefficients are applied. When the strip thickness is the same, as shown in Fig. 7(a), when the friction coefficient is 0.04, the contact contour maintains the circular shape, the plastic reduction along the whole deformation zone is more obvious, and there is no neutral zone. When the friction coefficient is 0.12, the contact profile presents a non circular arc shape, the plastic depression in the middle region of the deformation zone is very small, and a long neutral zone can be observed, which indicates that the deformation zone profile at this point in time has already appeared an obvious neutral zone. As the friction coefficient increases, the proportion of the neutral zone in the deformation zone increases, and the contact profile gradually changes from

a circular arc shape to a non circular arc shape. As shown in Fig. 7(b), when the friction coefficient is gradually increased from 0.04 to 0.12, the unit rolling pressure in the deformation zone gradually increases, and the unit rolling pressure is gradually changed from the traditional “peak” distribution to the elliptical distribution mentioned in Hertz theory.



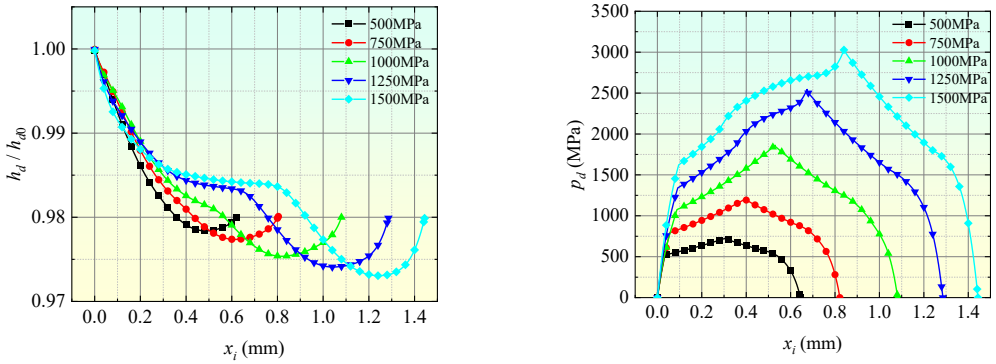
(a) Ratio of strip thickness in the deformation zone to the entry thickness

(b)unit rolling pressure

Fig. 7 Contour of deformation zone and unit rolling pressure for different friction coefficients

3.3 Different yield strengths

Five yield strengths of 500, 750, 1000, 1250 and 1500 MPa are selected, given the rolling process parameters: strip thickness is 0.16 mm, the undercutting rate is set to 2 %, the modulus of elasticity of rolls 0 and 0^x is 236,000 MPa, the Poisson's ratio of rolls 0 and 0^x is 0.3, the modulus of elasticity of the strip is 1,940,020 MPa, Poisson's ratio of the strip is 0.28, the strip entry and exit tensile stresses are 0.3, and the strip entry and exit tensile stresses are 0.4, 0.4, and 0.6. The strip modulus of elasticity is 194,020 MPa, strip Poisson's ratio is 0.28, strip entry and exit tensile stresses are 0 MPa, friction coefficient is 0.1, assuming that the incoming material cross-section shape is straight, rolls 1 and 1^x have a taper of 0 % and a taper length of 0 mm, and the ASU is not adjusted.



(a) Ratio of strip thickness in the deformation zone to the entry thickness

(b)unit rolling pressure

Fig. 8 Contours of deformation zone and unit rolling pressure at different yield strengths

Fig. 8 shows the contact deformation zone contours and the distribution of unit rolling pressure when different yield strengths are applied. At the same strip thickness, as shown in Fig. 8(a), when the strip yield strength is 500 MPa, the contact contour maintains a circular arc shape, and the plastic under pressure along the whole deformation zone is relatively obvious and there is no neutral zone.

When the yield strength of the strip is 1500 MPa, the contact profile presents a non circular arc shape, and the plastic depression in the middle region of the deformation zone is very small, and a long neutral zone can be observed, which indicates that the deformation zone profile at this time has already appeared an obvious neutral zone. As the yield strength of the strip is larger, the proportion of the neutral zone in the deformation zone is larger, and the contact profile gradually changes from a circular arc shape to a non circular arc shape. As shown in Fig. 8(b), when the strip yield strength is gradually increased from 500 MPa to 1500 MPa, the unit rolling pressure in the deformation zone gradually increases, and the unit rolling pressure is gradually changed from the traditional "peak"-shaped distribution to the elliptical distribution mentioned in Hertz theory. It is found that increasing the yield strength of the strip is equivalent to reducing the strip entry and exit tensile stresses at the same time, which is corroborated by the conclusions drawn from the analysis in subsection 3.1.

4. Conclusions

1. When rolling stainless steel thin strip, the working roll profile becomes non circular arc profile, the traditional rolling force calculation model will collapse when calculating, the rolls will be assumed as the premise of circular arc profile of the traditional rolling force model is no longer applicable, so this paper based on the non circular arc theory puts forward a new type of 20-high mill asymmetric flatness prediction model.

2. Compared with the traditional rolling force model based on non circular arc theory, the 20-high mill flatness prediction model can still operate stably when the strip thickness is thin, and the calculated flatness of the new model matches the measured flatness of the flatness instrument to a high degree, which verifies the accuracy of the model.

3. According to the influence of different tensile stress, friction coefficient and yield strength on the contour of rolling deformation zone and the unit rolling pressure, any factors that may lead to an increase in rolling pressure may lead to the appearance of a neutral zone in the deformation zone, and make the unit rolling pressure change gradually from the traditional "peak" distribution to the "peak" distribution of the unit rolling pressure, which is mentioned in the Hertz theory. Hertz theory mentioned in the elliptical distribution.

Acknowledgments

The work described herein was supported by the National Natural Science Foundation of China (No. U21A20118), the Natural Science Foundation of Hebei Province (No. E2023203065), the National Key Laboratory of Metal Forming Technology and Heavy Equipment, China National Heavy Machinery Research Institute Co., Ltd. (No. S2208100.W04), and Jinzhong University Research Funds for Doctor (JUD2026029).

Data availability

The datasets analyzed during the current study are not publicly available due to commercial confidentiality but are available from the corresponding author on reasonable request.

Declarations

Conflict of interest The authors declare no conflict of interest.

References

[1] J. Park, B. Kim, S. Han, Reinforcement learning with model-based assistance for shape control in sendzimir rolling mills, IEEE Transactions on Control Systems Technology, (2022).
[2] Y.-g. Hu, Y.-k. Choi, A fuzzy shape control method for stainless steel strip on Sendzimir rolling mill, Journal of Iron and Steel Research International, 18 (2011) 17-23.
[3] Z. Ren, T. Wang, W. Fan, Establishment of the tension stress model considering metal lateral flow for foil rolling, Meccanica, 54 (2019) 261-270.
[4] Z.-w. Yuan, H. Xiao, Plate shape control theory and experiment for 20-high mill, Journal of Iron and Steel Research International, 22 (2015) 996-1001.
[5] Z. Weimin, Q. Xiaofeng, Q. Haixia, W. Qiong, C. Wei, L. Fengbin, W. Hui, L. Feng, Numerical analysis of contact pressure between rolls of Sendzimir mill based on double influence function method and conjugate gradient techniques, Advances in Engineering Software, 176 (2023) 103388.
[6] J. Sun, M. Yan, M. Li, T. Hao, Study on setting method of flatness target curve of SUNDWIG 20-high mill considering target crown, The International Journal of Advanced Manufacturing Technology, 120 (2022) 6983-6992.
[7] Z. Ren, H. Xiao, T. Wang, Q. Huang, Plate profile control during ultra-thin strip rolling utilizing work roll edge contact, Journal of the Brazilian Society of Mechanical Sciences and Engineering, 41 (2019) 28.
[8] H.-l. Yu, X.-h. Liu, G.-T. Lee, Contact element method with two relative coordinates and its application to prediction of strip profile of a sendzimir mill, ISIJ international, 47 (2007) 996-1005.
[9] J.-m. Shin, S.-i. Han, J.-s. Kim, Development and experimental evaluation of strip shape prediction model for Sendzimir rolling mills, Journal of Iron and Steel Research International, 20 (2013) 25-32.
[10] HITCHCOCK J H. Report of ASME special research committee roll neck bearings[R]. New York：ASME Research Publictions,1935.
[11] D. Jortner, J.F. Osterle, C.F. Zorowski, An analysis of cold strip rolling, International Journal of Mechanical Sciences, 2 (1960) 179–194.
[12] STONE M D. Rolling of thin strip partII[J]. Iron and Steel Engineer,1956,33 (12)：55-76.
[13] E. Orowan, The Calculation of Roll Pressure in Hot and Cold Flat Rolling, ARCHIVE Proceedings of the Institution of Mechanical Engineers 1847-1982 (vols 1-196), 150 (1943) 140-167.
[14] K.L. Johnson, R.H. Bentall, The onset of yield in the cold rolling of thin strip, Journal of the Mechanics & Physics of Solids, 17 (1969) 253-264.
[15] N.A. Fleck, K.L. Johnson, M.E. Mear, L.C. Zhang, Cold rolling of foil, Proceedings of the Institution of Mechanical Engineers Part B Journal of Engineering Manufacture, 206 (1992) 119-131.
[16] N.A. Fleck, K.L. Johnson, Towards a new theory of cold rolling thin foil, International Journal of Mechanical Sciences, 29 (1987) 507-524.
[17] Y. Liu, W.H. Lee, Mathematical Model for the Thin Strip Cold Rolling and Temper Rolling Process with the Influence Function Method, Transactions of the Iron & Steel Institute of Japan, 45 (2006) 1173-1178.
[18] R. H., Le, and, P.F. M., Sutcliffe, A robust model for rolling of thin strip and foil, International Journal of Mechanical Sciences, 43 (2001) 1405-1419.
[19] T.A.M. Langlands, D.L.S. Mcelwain, A modified Hertzian foil rolling model: approximations based on perturbation methods, International Journal of Mechanical Sciences, 44 (2002) 1715-1730.
[20] T.A.M. Langlands, D.L.S. Mcelwain, S.A. Domanti, An approximate method for the solution of an influence function foil rolling model, International Journal of Mechanical Sciences, 46 (2004) 1139-1156.
[21] D. Wang, Y. Peng, H. Liu, A high-resolution high-speed rolling force model for cold strip temper

rolling mill, Journal of Plasticity Engineering, 15 (2008) 6.
[22] Z. Ren, H. Xiao, X. Liu, G. Wang, Experimental and theoretical analysis of roll flattening in the deformation zone for ultra-thin strip rolling, Ironmaking & Steelmaking, (2017) 1-8.
[23] Z. Ren, T. Wang, Y. Wang, Analysis of contact contour and contact pressure in deformation zone of ultra-thin strip rolling, Iron & Steel 53 (2018) 7.
[24] S. Jing-Na1, H. Hua-Gui1, D.U. Feng-Shan1, L. Xue-tong1, Y. University, Q. 066004, Hebei, China, L.o.M.M. Science, Technology, China), Nonlinear Finite Element Analysis of Thin Strip Temper Rolling Process, Journal of Iron and Steel Research(International), (2009).
[25] F.S. Feng, Jingna, Theoretical and experimental analysis of the deformation zone and minimum thickness in single-roll-driven asymmetric ultrathin strip rolling, The International Journal of Advanced Manufacturing Technology, 104 (2019).
[26] T. Dbouk, TWO-DIMENSIONAL ROLL BITE MODEL WITH LUBRICATION FOR COLD STRIP ROLLING, in: 6th International Conference on Tribology in Manufacturing Processes & Joining by Plastic Deformation, 2014.
[27] S.H. Lee, K.H. Lee, D.C. Ko, S.B. Lee, B.M. Kim, Development of Three-Dimensional Strip Profile Model for Thin-Foil Cold Rolling, Advances in Mechanical Engineering,2014, 312382-312382.
[28] K. Shohet, Roll bending methods of crown control in four-high plate mills, J. Iron and Steel Ins., (1968) 1088-1098.
[29] T. Ishikawa, Y. Tozawa, M. Nakamura, T. Kato, Fundamental study on the profile and shape of the rolled strip, in: International Conference on Steel Rolling, 1980, 772-783.
[30] G. Wang, S. Zhang, Matrix method for elastic deformation of rolls in a four-roll mill, Heavy Machinery, 8 (1982) 9-18.
[31] F. Ren, Z. Wang, Y. Jia, Rolling force model for 304 stainless steel ultra-thin strip based on mechanism and data fusion, Iron & Steel, 59 (2024) 64-76.